Selective Synthesis for light olefins from acetone over ZSM-5 zeolites with nano- and macro-crystal sizes

Teruoki Tago*, Hiroki Konno, Mariko Sakamoto, Yuta Nakasaka and Takao Masuda

Division of Chemical Process Engineering, Faculty of Engineering,

Hokkaido University, N13 W8, Kita-ku, Sapporo, Hokkaido, 060-8628, Japan

** corresponding author should be addressed*

e-mail: tago@eng.hokudai.ac.jp

tel:+81-117066551

fax: +81-117066552

Abstract

Production of light olefins such as ethylene, propylene and isobutylene from acetone was examined over ZSM-5 zeolites. These light olefins are produced from acetone over the acid sites of the zeolite via a series of consecutive reactions where olefins such as ethylene and propylene are obtained by cracking of isobutylene produced from aldol condensation products of acetone. Macro- and nano-sized ZSM-5 zeolites were prepared by conventional hydrothermal and emulsion methods, respectively, and the ZSM-5 zeolites with nearly the same acidity and BET surface area were obtained regardless of the crystal sizes. From SEM observations, the crystal sizes of the zeolites were approximately 2000 nm and 30-40 nm. These zeolites with different crystal sizes were applied to light olefins synthesis from acetone, and the effect of crystal size on catalytic activity and stability was investigated. As compared with the macro-seized zeolite, the nano-sized zeolite exhibited a high activity over a long lifetime. However, because the nano-sized zeolite possesses a large external surface area, undesirable reactions to form aromatics from the produced light olefins occurred on the acid sites located near the external surface. To inhibit aromatics formation, selective deactivation of the acid sites located near the outer surface of the zeolite was achieved via the catalytic cracking of silane (CCS) method using diphenyl silane (DP-silane). The CCS method was effective in deactivating the acid sites located near the external surface of the ZSM-5 zeolite. Moreover, the nano-size zeolite after the CCS treatment using DP-silane exhibited high olefins and low aromatics yields under high acetone conversion conditions.

Keywords

ZSM-5 zeolite, Crystal size, Light olefins

1. Introduction

Light olefins such as ethylene, propylene and isobutylene are some of the most important basic raw materials for the petrochemical industry, and demands for these olefins are increasing every year. Ethylene has been mainly produced by steam cracking of naphtha, and propylene is a by-product of the cracking process. Recently, alternative production methods and/or processes for these light olefins have been required due to wild ups and downs in oil prices. One promising candidate route for producing light olefins is an alcohol-to-olefins reaction (methanol-to-olefins [1,2], ethanol-to-olefins [3,4] and methanol-biomass mixture-to-hydrocarbons including olefins [5,6]), and another is olefin synthesis from acetone over solid-acid catalysts, where olefins such as ethylene, propylene and isobutylene are obtained from aldol condensation products of acetone [7-13], as shown in Fig. 1. Notably, a large amount of acetone is obtained as a by-product in the commercial cumene process. Moreover, acetone is selectively produced from biomass-derived tar (nonedible biomass such as sewage sludge [14], fermentation residue [15] and livestock excrement [16]) using an iron oxide composite catalyst. Accordingly, acetone conversion over solid-acid catalysts has become an attractive method for producing light olefins.

The light olefins are intermediate chemicals in the above-mentioned series of reactions, while aromatics and carbon solid (coke) are the terminal products. In order to increase the yield of light olefins, it is important to inhibit aromatics formation under high acetone conversion conditions. Because the molecular size of light olefins is smaller than that of aromatics, the spatial limitations within zeolite channels are expected not only to prevent the formation of aromatics, but also to provide effective reaction fields for increasing olefin yields. We have reported olefins synthesis from acetone over MFI (ZSM-5) [17] and BEA [18] zeolites. Unfortunately, when the reaction proceeds over acid sites located on the external surface of zeolite crystals, the zeolites exhibit a poor spatial limitation effect. Moreover, it is

likely that the conversion of the produced light olefins into aromatics readily occurs over the acid sites located on the external surface, leading to a short life time for the catalysts due to coke deposition. In order to prevent these non-desirable reactions, the acid sites located near the external surface of the zeolites need to be deactivated. Previously, we reported that acid sites near the external surface can be selectively de-activated using the catalytic cracking of silane (CCS) method, where SiO_2 units are formed selectively on the acid sites of the zeolite using organic silane compounds [19,20]. Moreover, it was determined that the selective deactivation of the acid sites near the external surface by the CCS method was effective in decreasing the aromatics yield and increasing the olefin yield [17,20].

As mentioned above, the zeolite in which the acid sites near the external surface are selectively deactivated by the CCS method is an effective catalyst for producing light olefins from acetone. Because the intermediate light olefins are mainly produced within the zeolite crystal, however, the diffusion resistances of the reactant acetone as well as the light olefins within the micropore affect the product yields and catalytic activity. In order to achieve a low diffusion resistance, two primary strategies have been proposed; one is the formation of meso-pores within zeolite crystals [21], and the other is the preparation of nano-crystalline zeolites [22,23]. Because the diffusion length for acetone and light olefins, assignable to the crystal size, decreases in nano-sized zeolite, application of nano-sized zeolite is effective in achieving faster mass transfer of these hydrocarbons within the micropore.

The main objective of this study was to develop a zeolite catalyst for light olefins synthesis from acetone. First, ZSM-5 zeolites with different crystal sizes were applied to light olefins synthesis. In order to investigate the effect of the crystal sizes of ZSM-5 on olefin yield and catalyst lifetime in detail, zeolites with different crystal sizes needed to be prepared with the same acidity and crystallinity. We have reported a preparation method for nano-sized zeolites via hydrothermal synthesis in a water/surfactant/organic solvent (emulsion method [24-27]). The nano-sized ZSM-5 zeolite was prepared by the emulsion method and the catalytic activity

and product yields were compared with a macro-sized ZSM-5 zeolite prepared by a conventional hydrothermal method. Moreover, in order to inhibit the excessive conversion of produced olefins into aromatics, the CCS method was applied for the selective deactivation of acid sites located near the external surface of the zeolites, and the effect of the selective deactivation of acid sites in the zeolites with different crystal sizes on catalytic activity and life time were examined. Finally, the relationship between the yields of each olefin (ethylene, propylene and butylene) and acetone conversion was investigated using the nano-sized ZSM-5 zeolite prior to and after CCS treatment.

2. Experimental

2.1. Preparation of nano- and macro-sized ZSM-5

A nano-size ZSM-5 (MFI-type zeolite) zeolite was prepared via hydrothermal synthesis in a water/surfactant/organic solvent. A water solution containing Si and Al sources was obtained by hydrolyzing each metal alkoxide (tetraethylorthosilicate and aluminum triisopropoxide, Wako Pure Chemical Industries, Ltd.) with a dilute tetrapropyl ammonium hydroxide/water solution at room temperature. The tetrapropyl ammonium hydroxide molecules act as organic structure directing agents (OSDA). The molar ratios of Si to OSDA and the Si concentration in water were 3.3 and 1.0 mol/L, respectively. The molar ratio of Si to Al was 80 and 200. Sodium hydroxide was used as a Na source. The starting water solution was stirred for 24 h, and then 10 cc was slowly added to the surfactant/organic solvent solution (70 cc). The mixture was magnetically stirred at 323 K for 1 h. Polyoxyethylene(15)oleylether (Nikko Chemical, denoted as O-15 hereafter) and cyclohexane (Wako, C_6H_{12}) were employed as the surfactant and organic solvent, respectively. The concentration of O-15 ([O-15]) in the surfactant/organic solvent was 0.5 mol/L. Next, the mixture was placed in a Teflon sealed

stainless steel bottle, heated to 393 K and then held at this temperature for 24 h with stirring to yield ZSM-5 nanocrystals. This method is referred to hereafter as the emulsion method.

A macro-sized ZSM-5 zeolite was also prepared using a conventional hydrothermal technique. The water solution containing Si and Al sources without surfactant/organic solvent was poured into a Teflon-sealed stainless bottle and the preparation was carried out at a high temperature of 473 K for 48 h. Si concentration was 0.3 mol/L.

For both methods, the precipitate of the ZSM-5 zeolite thus obtained was centrifuged, washed thoroughly with 2-propanol, dried at 373 K overnight, and then calcined under an air flow at 773 K to remove the surfactant and the OSDA. The ZSM-5 zeolites were treated with an ammonium nitrate solution (0.5 mol/L) at 353 K to obtain NH_4-type ZSM-5 through the exchange of Na^+ cations with NH_4^+ cations.

2.2. Selective deactivation of acid sites of the zeolites using the CCS method

Selective de-activation of the acid sites located near the external surface of the ZSM-5 zeolites was achieved using the catalytic cracking of silane method (CCS method). The CCS treatment was carried out in a fixed bed reactor loaded with 0.5 g of zeolites at atmospheric pressure. The zeolite was exposed to silane compound vapor at 373 K in a N_2 stream, and the feed of the silane compound was then stopped to remove the physically adsorbed silane compounds on the zeolite surface. The sample was heated to 823 K in a N_2 stream to decompose the silane compounds adsorbed on the acid sites, leading to formation of silicon-coke composites. Finally, N_2 gas flowing around the zeolite was switched to air, and the temperature of the reactor was held at 823 K in an air stream for 60 min to oxidized silane-coke compounds to SiO_2 units on each acid site. Thus, the acid sites where the silane compounds were adsorbed were deactivated by the SiO_2 units. The sequence of the procedure described above was repeated three times. Since the molecular diameter of diphenyl silane

(DP-silane) is almost the same as the pore size of ZSM-5 zeolite, our previous research revealed that the CCS method using DP-silane is effective in de-activating the acid sites located near the external surface of ZSM-5 zeolite crystals. In this study, therefore, DP-silane was employed as the silane compound for the selective deactivation of the acid sites of ZSM-5 zeolites.

2.3. Characterization of zeolite

The morphology and crystallinity of the obtained materials were investigated using a field-emission scanning electron microscope (FE-SEM; JEOL JSM-6500F) and an X-ray diffractometer (XRD; JEOL JDX-8020). The N_2 adsorption and desorption isotherms of the obtained materials were measured (BEL Japan, Inc., Belsorp mini), and the total surface area, external surface area and micropore volume were calculated using the BET and t-methods [28]. The acidity of the obtained samples was evaluated via the ac-NH_3-TPD method [29]. In the TPD experiment, the carrier gas was 1.0 % NH_3 (balance He), the heating rate was 5 K min^{-1}, and the temperature range was 373 to 823 K. The desorption of NH_3 molecules from the acid sites of the zeolite was measured under a 1.0% NH_3-He atmosphere so that the TPD profile could be measured under complete adsorption equilibrium conditions, which is referred to as the ac–NH3–TPD method.

2.4. Olefin synthesis from acetone over ZSM-5 zeolite

The ZSM-5 zeolite described above was pelletized without any binder, crushed and sieved to yield samples ca. 0.3 mm in diameter that were used as catalysts for the synthesis of isobutylene from acetone. The olefin synthesis was carried out using a fixed bed reactor under a N_2 stream (60 cc/min) at atmospheric pressure and a temperature of 673 K with a *W*/*F*

(weight ratio of catalyst (g) to acetone feed rate (g/h)) of 0.5 kg-cat/(kg-acetone/h). ZSM-5 zeolites with different crystal sizes prior to and after CCS treatment were employed as catalysts. The reaction products were analyzed using online gas chromatography (Shimadzu Co. Ltd., GC-14A) with a porapak-Q column and FID detector.

3. Results and Discussion

3.1 Olefins synthesis from acetone over ZSM-5 zeolites with different Si/Al ratios

Olefins synthesis from acetone over ZSM-5 zeolites with different Si/Al ratios was carried out in order to investigate the effect of acid site density on the product distributions. The change in acetone conversion with time and the relationship between the product yields and the conversion using H-ZSM-5 zeolites with different Si/Al ratios (80 and 200) are shown in Figures 2(a) and 2(b), respectively. In order to compare the effect of acid site density on the catalytic activities, the experiments were carried out using a constant amount of Al in the catalyst beds by changing the catalyst weight (W/F=0.2 in Si/Al=80 and W/F=0.5 in Si/Al=200).

Olefins (ethylene, propylene and isobutene) and aromatics were primarily produced from acetone over the ZSM-5 zeolite catalysts. Isobutene was first produced from aldol condensation products of acetone [5-11], followed by production of propylene, ethylene and aromatics over the acid sites. These light olefins are intermediate chemicals in the series of reactions with aromatics and coke as terminal products. As shown in Fig. 2(a), although the number of Al atoms loaded in the catalyst beds was constant, the change in acetone conversion with time on stream was different. Since the acid site density of the ZSM-5 zeolite with a Si/Al ratio of 80 was higher than that of the zeolites with a Si/Al ratio of 200, it was considered that excessive reaction to produce aromatics from two or three olefin molecules progressed over

the acid sites in the zeolite with a Si/Al ratio of 80, leading to coke formation and deactivation. In contrast, as shown in Fig. 2(b), the relationships between acetone conversion and yields of olefins and aromatics were similar regardless of the different Si/Al ratio. Because the production of these light olefins and aromatics proceeded readily due to the strong acidity of the H-ZSM-5 zeolite, it was concluded that the product distribution in the series of reactions shown in Fig. 1 depends on the acetone conversions. In this study, the ZSM-5 zeolites with a Si/Al ratio of 80 were applied to olefins synthesis from acetone. In order to investigate the effect of crystal size on catalytic activity, ZSM-5 zeolites with different crystal sizes were prepared and used as catalysts for olefins synthesis.

3.2 Preparation of ZSM-5 zeolites with different crystal sizes

In order to accurately investigate the effect of crystal size on the catalytic performance of zeolites in olefin synthesis from acetone, it was necessary to prepare zeolites with the same acidity and crystallinity. For this purpose, ZSM-5 zeolites with different crystal sizes were prepared by conventional and emulsion methods. The Si/Al ratio in the synthetic solution was 80. X-ray diffraction patterns and FE-SEM photographs of the obtained ZSM-5 zeolites can be seen in Figures 3 and 4, respectively. The XRD patterns of these samples showed peaks corresponding to an MFI-type zeolite. Although aggregation of the zeolites was observed, nanocrystals with sizes of approximately 30-40 nm could be obtained by the emulsion method (Fig. 4(a)). On the other hand, with the conventional method, zeolites with crystals sizes of approximately 2000 nm were obtained. The zeolites with the crystal sizes of 30-40 nm and 2000nm are hereafter denoted as nano-sizes and macro-sizes zeolites, respectively.

The SEM observation and XRD analysis demonstrated the preparation of ZSM-5 zeolites with different crystal sizes. In order to investigate in detail zeolitic properties such as micropore volume, surface area and acidity, N_2 adsorption isotherms and NH_3-TPD profiles of

the zeolites were measured (Figs 5 and 6, respectively). BET and external surface areas and micropore volumes of these zeolites calculated from the N_2 adsorption isotherms using the BET and t-methods are listed in Table 1.

The steep increase in the amount of adsorbed N_2 in the region of low relative pressure (P/P_0) followed by the flat curve corresponds to the filling of the micropores. As listed in Table 1, the micropore volumes of these samples were approximately 0.13-0.17 cm^3/g, values which are nearly the same as that of MFI zeolite, indicating that these zeolites contained a considerable micropores volume in their framework. Moreover, while the external surface area of the nano-sized zeolite was much larger than that of the macro-sized zeolite due to the difference in the crystal sizes, the nano-sized zeolite exhibited almost the same BET surface area of 370 m^2/g as the macro-sized zeolite. Accordingly, ZSM-5 zeolites with the same BET surface area could be obtained despite their different crystal sizes. The mesopore in the size range from 2 to 10 nm calculated by BJH method were existed in nano- and macro-sized ZSM-5 zeolites. Because the mesopores and their surface were composed of pore spaces among the zeolite crystals, the mesopore volume in nano-sized ZSM-5 zeolite was larger than that in macro-sized zeolite. In contrast, because the molecular sizes of light olefins and acetone were much smaller than the mesopore sizes, it was considered that the micropore within the zeolite crystal affected the diffusion of these hydrocarbon molecules.

The NH_3 desorption peak observed at temperatures above 600 K is associated with strong acid sites (Fig. 6). The TPD profiles of the nano-and macro-sized zeolites with Si/Al ratio of 80 exhibited almost the same peak position and area, indicating that these zeolites possessed almost the same acidity regardless of the different crystal sizes. In conclusion, zeolites with the same BET surface area and acidity could be obtained regardless of their crystal sizes.

3.3 Effect of crystal sizes of ZSM-5 zeolites on light olefins synthesis from acetone

Olefin synthesis from acetone was carried out over ZSM-5 zeolites with different crystal sizes. The changes in acetone conversion, product selectivity and olefin yield with reaction time over the macro- and nano-sized zeolites can be seen in Figs. 7 and 8, respectively. The reactions were run at 673 K with a *W*/*F* of 0.5 kg-cat/(kg-acetone/h).

Although the zeolites used as catalysts possessed nearly the same crystallinity and acidity, the change in acetone conversion with time was very different for the two zeolites. With the macro-sized zeolite (Fig, 7), conversion decreased with time most likely due to coke deposition on the acid sites. It is believed that a large diffusion resistance for the reactant acetone and intermediate olefins within the crystals exists in the macro-sized zeolite. Thus the series of reactions of acetone likely occurred on the acid sites near the external surface of the crystal where plugging of the pore mouth easily progressed due to coke deposition. Moreover, the small external surface area of the macro-sized zeolite intensified the decrease in the catalytic activity due to the pore plugging. While the selectivity for olefins seemed to increase with time, the increase resulted from an increase in isobutylene formation from acetone, indicating that the series of reactions was terminated at the production of iso-butylene.

In contrast, the nano-sized zeolite, as shown in Fig. 8, exhibited stable and high activity as compared with the macro-sized zeolite. These differences in catalytic activity and stability resulted from the difference in the crystal sizes. As the crystal size decreased, the diffusion length for the intermediates decreased and the external surface area (and surface-to-volume ratio, S/V) increased, leading to the stable and high activity of the nano-sized zeolite. However, the selectivity for aromatics was much higher than for the other products in the nano-sized zeolite. When the acetone conversion proceeds over the acid sites located on the pore surface within the crystals, the light olefins are selectively produced due to the narrow pore spaces (0.56 nm × 0.53 nm) of the MFI zeolite. Because the nano-sized zeolite possesses a large external surface area compared to the macro-sized zeolite, however, it was concluded that the

produced olefins easily reacted with each other on the acid sites located on the external surface of the crystal, where there is no spatial limitation for formation of aromatics. In order to increase the olefin yield, it was therefore necessary to inhibit aromatic formation on the acid sites located near the external surface.

3.4 Deactivation of acid sites located near the external surface and its effect on catalytic performance

Light olefins such as ethylene, propylene and isobutylene are intermediate chemicals in the series of reactions, and aromatics and coke are terminal products mainly formed on the acid sites located near the external surface. Accordingly, inhibition of aromatics and coke formation near the external surface, in addition to a low diffusion resistance to the intermediate olefins within the micropore of the zeolite, is required to achieve high olefin yield. For this purpose, selective deactivation of the acid sites located near the external surface of the nano-sized zeolite was achieved with diphenyl silane (DP-silane) using CCS method.

The *ac*-NH_3-TPD profiles of the nano-sized zeolite prior to and after CCS treatment can be seen in Fig. 9. As shown in the figure, the amount of NH_3 desorbed from the strong acid sites decreased after CCS treatment due to the formation of silica units on the acid sites. The amount of NH_3 desorbed from the strong acid sites of the zeolites prior to and after CCS treatment were 0.17 mol/kg and 0.12 mol/kg, respectively, indicating that approximately 30% of the strong acid sites were deactivated by CCS treatment. On the other hand, as listed in Table 1, the ratio of the external surface area (78.2 m^2/g) to BET surface area (370 m^2/g) in the nano-seized ZSM-5 zeolite prior to CCS treatment was approximately 20%. In our previous research, we found that, because the molecular size of DP-silane is nearly the same as the pore diameter of ZSM-5 zeolite, the acid sites located on the external surface as well as near the external surface are selectively deactivated in ZSM-5 zeolite using the CCS method with

DP-silane. Accordingly, the difference between the decrease in the amount of acid sites (30%) and the ratio of external surface area (20%) was attributed to the deactivation of acid sites inside the pore near the external surface.

Importantly, while acid sites located on and/or near the external surface of the ZSM-5 zeolite were deactivated using the CCS method with DP-silane, acid sites (micropore spaces) deep inside the zeolite were expected to remain. In order to confirm this assumption, N_2 adsorption isotherms of the nano-sized ZSM-5 zeolite prior to and after CCS treatment were measured (Figure 10). BET and external surface areas and micropore volumes of these zeolites calculated from the N_2 adsorption isotherms using the BET and t-methods are also listed in Table 1. Although the BET and external surface areas were slightly changed due to silica formation on the acid sites, the N_2 adsorption isotherms and micro pore volumes were nearly unchanged. Accordingly, it was considered that the micropore space deep inside the nano-sized zeolite was maintained after CCS treatment.

Olefin synthesis from acetone over the nano-sized zeolites prior to and after CCS treatment was then carried out. The change in acetone conversion with time is shown in Figure 11 (reaction runs at 673 K with a W/F of 0.5 kg-cat/(kg-acetone/h)). In order to compare the effect of crystal sizes on catalytic activity, the experiments were also carried out under the same conditions using the macro-sized zeolite after CCS treatment with DP-silane.

In the macro-sized zeolite after CCS treatment, not only was the initial catalytic activity low as compared with the zeolite prior to CCS treatment, but the activity decreased drastically with time on stream. As discussed above, the acid sites located near the external surface were selectively deactivated by the formation of silica units during the CCS treatment. Moreover, since it was considered that the acetone conversion progressed under a diffusion-limitation condition in the macro-sized zeolite, the reaction mainly occurred on the acid sites near the external surface, which were already deactivated by the CCS treatment. Accordingly, the selective deactivation of acid sites using the CCS method was inappropriate for the zeolite

catalyst with a large diffusion resistance.

In the nano-sized zeolite, although approximately 30% of the acid sites were deactivated by the CCS treatment, the catalytic activity was only slightly decreased as compared with the nano-sized zeolite prior to CCS treatment. Moreover, both the nano-sized zeolites exhibited higher catalytic activity than the macro-sized zeolite. While acetone conversion in the macro-sized zeolite decreased to approximately 30% after 500 min, at that time the conversion for the nano-sized zeolites was above 80%, and decreased to 30% after approximately 2500 min. The long lifetime of both of the nano-sized zeolites was attributed to the low diffusion resistance for the reactant acetone and the intermediate olefins and the large external surface area. Accordingly, the use of nano-sized ZSM-5 zeolites in olefin synthesis is effective in increasing the catalyst life time.

The relationship between acetone conversion and total product yields is shown in Fig. 12(a) and typical results with almost the same conversions were listed in Table 2. The experimental results shown in Fig. 11 were used as the values for acetone conversion, and as discussed previously acetone conversion decreased with increasing reaction time. As the acetone conversion decreased, the total aromatics yield decreased significantly, while the total olefins yield remained constant at approximately 30-40 C-mol% for acetone conversions above 50% and then slightly decreased. The difference in the changes in yield with conversion for the aromatics and olefins was attributed to the termination of the series of reactions at the olefin production stages shown in Fig. 1.

In the zeolite prior to CCS treatment, the yield of aromatics was much higher than that for the olefin, because more than 20% of the acid sites existed near the external surface, where there is no spatial limitation for formation of aromatics, causing the excessive reactions to produce aromatics from olefins. In contrast, the zeolite after CCS treatment exhibited higher olefins and lower aromatics yields than the zeolite prior to CCS treatment, indicating that the selective deactivation of the acid sites near the external surface affected product yields.

The relationship between the olefins yield and acetone conversion can be seen in Fig. 12(b). While the zeolites produced nearly the same yields of ethylene regardless of the CCS treatment, the zeolite after CCS treatment exhibited higher yields of propylene and isobutylene in the high acetone conversion region above 80% (reaction time within 500 min) than the zeolite prior to CCS treatment. The difference in the sum of the yields of propylene and iso-butylene between the zeolites prior to and after CCS treatment ranged from 10 to 15 C-mol% in the high acetone conversion region, and these values were nearly the same as the difference in the aromatics yield between the zeolites prior to and after CCS treatment (Fig. 12(a)). Accordingly, it was concluded that the selective deactivation of the acid sites near the external surface effectively inhibited the production of aromatics from light olefins. The maximum yield of light olefins such as ethylene, propylene and isobutylene reached approximately 45 C-mol%.

3.5 Reaction mechanism for production of propylene, ethylene and aromatics

Although isobutylene was produced by decomposition of aldol condensation products of acetone as shown in Fig. 1, production of propylene, ethylene and aromatics was unclear. Accordingly, the reaction pathways for propylene, ethylene and aromatics production were investigated. Fig. 13 shows the relationship between acetone conversion and product yields (13(a) aromatics and 13(b) aliphatics yields) during the acetone to olefins reaction over the nano-sized zeolite after CCS treatment shown in Fig. 12. The sum of the aromatics yields (benzene, toluene, xylene and tri-methyl benzene) shown in Fig. 13(a) was corresponding to the total aromatics yield shown in Fig. 12, and poly-alkyl benzene with the carbon number above 10 yielded less than 3 C-mol%.

Major products in aromatics and aliphatics were xylene, tri-methyl benzene (Fig. 13(a)) and butane (Fig. 13(b)), respectively. As shown in Fig. 13(b), although C_{5+} aliphatics, which were corresponding to others in Figs. 7 and 8, could not be identified, butane and C_{5+} aliphatics were observed and the yields of methane, ethane and propane were less than 0.2 C-mol%. It

was considered that butane was produced by hydride transfer between C_4 carbenium ion and olefin.

As can be seen from Fig. 13(a), the order of aromatics yields was as follows: xylene, tri-methyl benzene, toluene and benzene. Moreover, it was found that the dependency of these aromatics yields on acetone conversion exhibited almost the same tendency as the yields of propylene, ethylene and C_{5+} aliphatics, where these yields decreased with decreasing acetone conversion and reached to almost zero at the acetone conversion of approximately 30%. Accordingly, it was considered that a causal relationship existed among the production of C_{5+} aliphatics, aromatics and light olefins. Based on the simultaneous decrease in these yields with acetone conversion, possible reaction pathways for propylene, ethylene and aromatics were shown in Fig. 14. It is considered that the produced iso-butylene reacts with each other to produce C_8 aliphatics followed by cyclization/cracking to form C_8 aromatics (xylene), propylene and C_5 aliphatics. When C_5 aliphatics reacts with propylene and isobutylene, it is considered that C_8 and C_9 aromatics corresponding to xylene and tri-methyl benzene, respectively, are produced. Tri-methyl benzene is decomposed into ethylene and toluene [30], reported by Joensen in methanol conversion over H-ZSM-5. In this hypothesized reaction pathways, it is considered that propylene, xylene and tri-methyl benzene are major products from isobutylene, which is in good agreement with experimental results shown in Figs. 12 and 13.

Finally, as shown in Fig. 1, there are two reaction pathways where dimmer and trimmer of acetone are decomposed to produce isobutylene. In MFI type zeolite, the simultaneous decreases in the yields of propylene, ethylene and aromatics with acetone conversion were observed, whereas isobutylene continued to be produced (only isobutylene was generated), as shown in Fig. 12. In contrast, in our previous research using ion-exchanged BEA zeolite [18], continuous production of isobutylene and aromatics were observed, where the yield of isobutylene reached to 55 C-mol% (isobutylene selectivity was above 90 carbon% in light

olefins). Since trimmer of acetone (pholone and iso-pholone) could be formed in BEA zeolite (12-membered rings), iso-butylene and aromatics were observed, where cyclic compound of iso-pholone was converted into aromatics. In contrast, when using MFI zeolite in this study, it is considered that isobutylene is formed by the decomposition of diacetone alcohol (dimmer), not the decomposition of trimmer of acetone (pholone and iso-pholone), due to spatial limitation of MFI zeolite with 10-membered rings.

As discussed above, it is considered that xylene, tri-methyl benzene and toluene are formed during production of propylene and ethylene. Because the acid sites near the external surface of MFI zeolite were de-activated by CCS method, the yields of aromatics decreased due to inhibition of aromatics formation near the external surface, and these aromatics were produced mainly within ZSM-5 crystals around cross sectional spaces.

4. Conclusions

Production of light olefins such as ethylene, propylene and isobutylene from acetone was examined over ZSM-5 zeolites with different crystal sizes. Macro- and nano-sized ZSM-5 zeolites were prepared via conventional hydrothermal and emulsion methods, respectively. From SEM observations, the crystal sizes of the zeolites were determined to be approximately 2000 nm and 30-40 nm, and these ZSM-5 zeolites possessed almost the same acidity and BET surface area regardless of the crystal sizes. As compared with the macro-sized zeolite, the nano-sized zeolite exhibited high activity with a long lifetime. This improved performance resulted from a low diffusion resistance for the acetone and light olefins. Because the nano-sized zeolite possesses a large external surface area, however, undesirable reactions to form aromatics from the produced light olefins easily occurred on the acid sites located near the external surface. Accordingly, in order to inhibit the aromatics formation, selective deactivation of the acid sites located near the outer surface of the zeolite was achieved using

the CCS method with DP-silane. The nano-sized zeolite after the CCS treatment using DP-silane exhibited a high olefins yield as well as a low aromatics yield under high acetone conversion conditions.

Acknowledgments

This work was supported by the green sustainable chemistry project of New Energy and Industrial Technology Development Organization (NEDO). This work was also partly supported by Grant-in-Aid for Scientific Research (No. 22560755) of Education, Culture, Sports, Science and Technology of Japan.

References

[1] M. Stocker, Micropor. Mesopor. Mater. 29 (1999) 3-48.

[2] F. J. Keil, Micropor. Mesopor. Mater. 29 (1999) 49-66.

[3] I. M. Dahl, R. Wendelbo, A. Andersen, D. Akporiaye, H. Mostad, T. Fuglerud, Micropor. Mesopor. Mater. 29 (1999) 159-171.

[4] H. Oikawa, Y. Shibata, K. Inazu, Y. Iwase, K. Murai, S. Hyodo, G. Kobayashi, T. Baba, Appl. Catal. A 312 (2006) 181-185.

[5] U. V. Mentzel, M. S. Holm, Appl. Catal. A 396 (2011) 59-67.

[6] A. G. Gayubo, B. Valle, A. T. Aguayo, M. Olazar, J. Bilbao, Ind. Eng. Chem. Res. 49 (2010) 123-131.

[7] J. Novakova, L. Kubelkova, Z. Dolejsek, J. Molec. Catal. 39 (1987) 195-202.

[8] L. Kubelkova, J. Cejka, J. Novakova, Zeolite 11 (1991) 48-53.

[9] L. Kubelkova, J. Novakova, Zeolite 11 (1991) 822-826.

[10] A. I. Biaglow, J. Sepa, R. J. Gorte, D. White, J. Catal. 151 (1995) 373-384.

[11] A. G. Panov, J. T. Fripiat, J. Catal. 178 (1998) 188-197.

[12] A. Panov, J. J. Fripiat, Langmuir 14 (1998) 3788-3796.

[13] W. G. Song, J. B. Nicholas, J. F. Haw, J. Phys. Chem. B 105 (2001) 4317-4323.

[14] E. Fumoto, Y. Mizutani, T. Tago, T. Masuda, Appl. Catal. B, Environ. 68 (2006) 154-159.

[15] S. Funai, Y. Satoh, Y. Satoh, K. Tajima, T. Tago, T. Masuda, Top. Catal. 53 (2010) 654-658.

[16] S. Funai, T. Tago, T. Masuda, Catal. Today 164 (2011) 443-446.

[17] T. Tago, M. Sakamoto, K. Iwakai, H. Nishihara, S. R. Mukai, T. Tanaka, T. Masuda, J. Chem. Eng. Jpn. 42 (2009) 162-167.

[18] T. Tago, H. Konno, S. Ikeda, S. Yamazaki, W. Ninomiya, Y. Nakasaka, T. Masudaa, Catal. Today 164 (2011) 158-162.

[19] T. Masuda, N. Fukumoto, M. Kitamura, S. R. Mukai, K. Hashimoto, T. Tanaka, T. Funabiki, Micropor. Mesopor. Mater. 48 (2001) 239-245.

[20] T. Tago, K. Iwakai, K. Morita, K. Tanaka, T. Masuda, Catal. Today, 105 (2005) 662–666.

[21] S. van Donk, A. H. Janssen, J. H. Bitter, K. P. de Jong, Catal. Rev., 45 (2003) 293-319.

[22] L. Tosheva, V. P. Valtchev, Chem. Mater. 7 (2005) 2494-2513.

[23] S. C. Larsen, J. Phys. Chem. C 111 (2007) 18464-18474.

[24] T. Tago, M. Nishi, Y. Kono, T. Masuda, Chem. Lett. (2004) 1040-1041.

[25] T. Tago, K. Iwakai, M. Nishi, T. Masuda, J. Nanosci. Nanotechnol. 9 (2009) 612-617.

[26] T. Tago, D. Aoki, K. Iwakai, T. Masuda, Top. Catal. 52 (2009) 865-871.

[27] K. Iwakai, T. Tago, H. Konno, Y. Nakasaka, T. Masuda, Micropor. Mesopor. Mater. 141 (2011) 167–174.

[28] Y. S. Bae, A. O. Yazaydin, R. Q. Snurr, Langmuir 26 (2010) 5475-5483.

[29] T. Masuda, Y. Fujikata, S. R. Mukai, K. Hashimoto, Appl. Catal., A 165 (1997) 57-72.

[30] M. Bjorgen, S. Svelle, F. Joensen, J. Nerlov, S. Kolboe, F. Bonino, L. Palumbo, S. Bordiga, U. Olsbye, J. Catal. 249 (2007) 195-207.

Figure and Table captions

Figure 1. Reaction pathways for Olefins synthesis from acetone over solid-acid catalyst

Figure 2. (a) Change in acetone conversion with time and (b) relationship between product yield and conversion using H-ZSM-5 zeolites with different Si/Al ratios (80 and 200).

Figure 3. X-ray diffraction patterns of nano- and macro-sized ZSM-5 zeolites.

Figure 4. FE-SEM photographs of (a) nano- and (b) macro-sized ZSM-5 zeolites.

Figure 5. Nitrogen adsorption isotherms of nano- and macro-sized ZSM-5 zeolites.

Figure 6. NH_3-TPD profiles of nano- and macro-sized ZSM-5 zeolites.

Figure 7. Changes in acetone conversion, products selectivity and olefin yield with reaction time over the macro-sized zeolite. The reaction was run at 673 K with a *W*/*F* of 0.5 kg-cat/(kg-acetone/h).

Figure 8. Changes in acetone conversion, product selectivity and olefin yield with reaction time over the nano-sized zeolite. The reaction was run at 673 K with a *W*/*F* of 0.5 kg-cat/(kg-acetone/h).

Figure 9. NH_3-TPD profiles of the nano-sized zeolite prior to and after CCS treatment.

Figure 10. Nitrogen adsorption isotherms of the nano-sized zeolite prior to and after CCS treatment.

Figure 11. Change in acetone conversion with time over nano- and macro-sized zeolites prior to and after CCS treatment. The reactions were run at 673 K with a *W*/*F* of 0.5 kg-cat/(kg-acetone/h).

Figure 12. Relationship between acetone conversion and product yields ((a) total olefins and

aromatics yields and (b) each olefin yield) during the acetone to olefins reaction over the nano-sized zeolite prior to and after CCS treatment. The reactions were run at 673 K with a *W*/*F* of 0.5 kg-cat/(kg-acetone/h).

Figure 13. Relationship between acetone conversion and product yields ((a) aromatics yields and (b) aliphatics yields) during the acetone to olefins reaction over the nano-sized zeolite after CCS treatment shown in Fig. 12.

Figure 14. Possible reaction pathways for propylene, ethylene and aromatics from isobutylene.

Table 1. BET and external surface areas and micropore volumes of prepared zeolites.

Table 2. Acetone conversion and product yields over macro- and nano-sized zeolites prior to and after CCS treatment.

Table 1. BET and external surface areas and micropore volumes of prepared zeolites.

sample	S_{BET} ($m^2\ g^{-1}$)	S_{ext} ($m^2\ g^{-1}$)	V_m ($cm^3\ g^{-1}$)
Macro-sized ZSM-5	371	12.6	0.17
Nano-sized ZSM-5 (Prior to CCS)	370	78.2	0.13
Nano-sized ZSM-5 (After CCS)	345	85.4	0.12

S_{BET} : surface area by BET method, S_{ext} : external surface area by t-method

V_m : micropore volume by t-method

Table 2. Acetone conversion and product yields over macro- and nano-sized zeolites prior to and after CCS treatment.

Catalysts	Time [min]	Conversion (%)	Olefins yield (C-mol%)				Aromatics yield (C-mol%)
			C_2=	C_3=	C_4=	Total olefins	
Macro-sized ZSM-5 (Prior to CCS)	195	65.0	2.9	10.4	14.6	27.9	27.0
	385	31.9	0.3	1.7	19.6	21.6	5.5
Macro-sized ZSM-5 (After CCS)	80	58.5	0.6	3.1	26.3	30.0	17.1
	380	32.8	0.1	0.4	27.0	27.5	2.1
Nano-sized ZSM-5 (Prior to CCS)	60	99.7	6.1	15.5	6.6	28.2	54.3
	1440	56.3	1.0	7.3	23.0	31.3	21.1
	2110	35.8	0.2	1.2	26.0	27.4	7.9
Nano-sized ZSM-5 (After CCS)	60	97.6	6.8	25.8	12.7	45.3	35.6
	1170	58.9	0.7	5.2	27.0	32.9	9.6
	2110	34.4	0.2	0.8	26.3	27.3	1.4

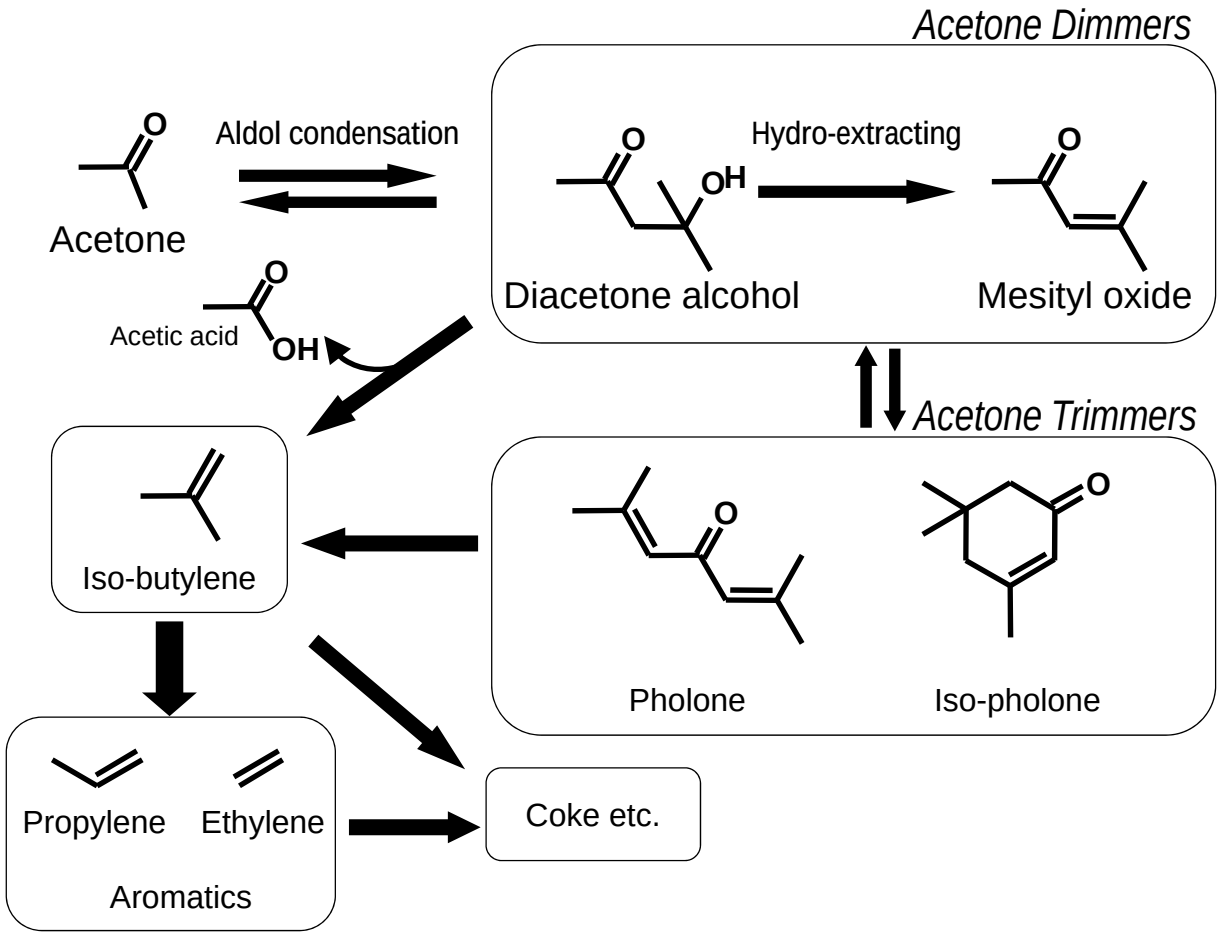

Figure 1. Reaction pathways for Olefins synthesis from acetone over solid-acid catalyst

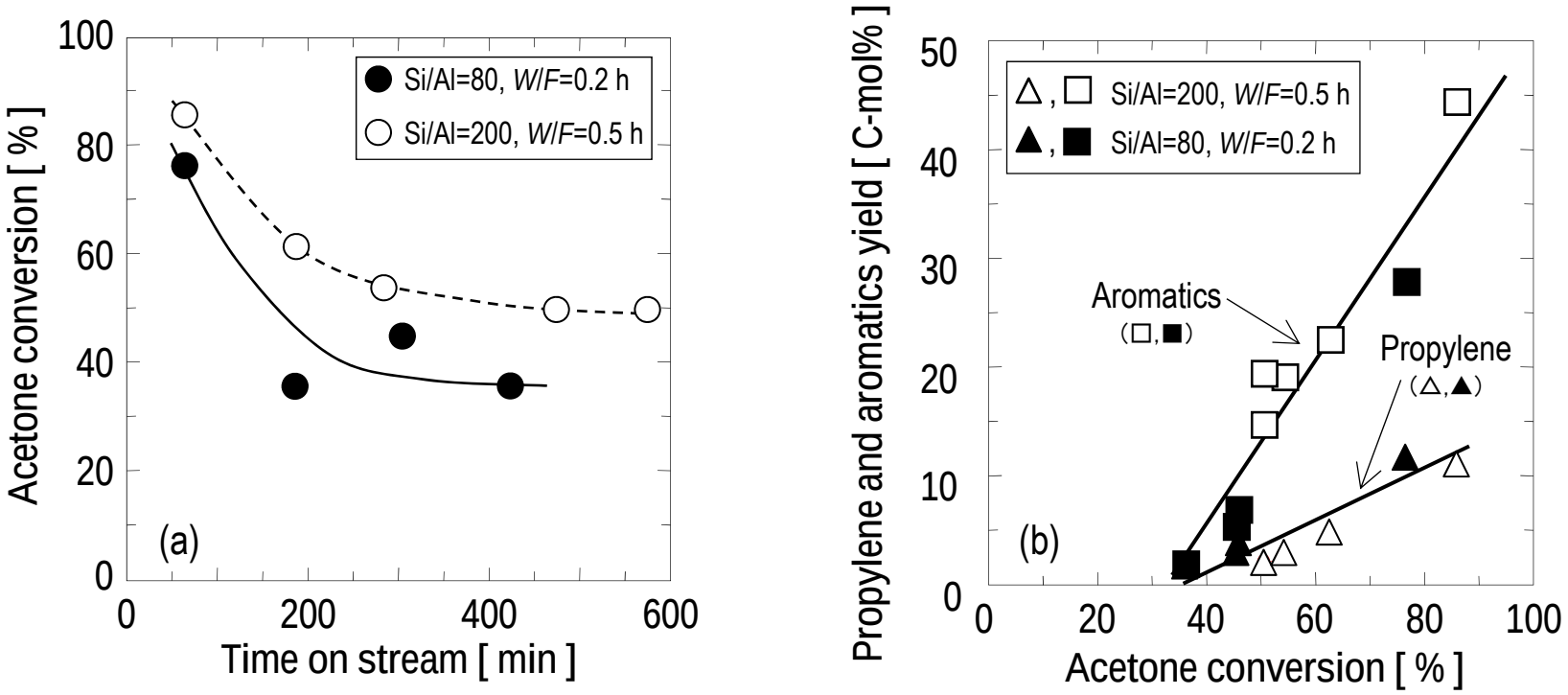

Figure 2. (a) Change in acetone conversion with time and (b) relationship between product yield and conversion using H-ZSM-5 zeolites with different Si/Al ratios (80 and 200).

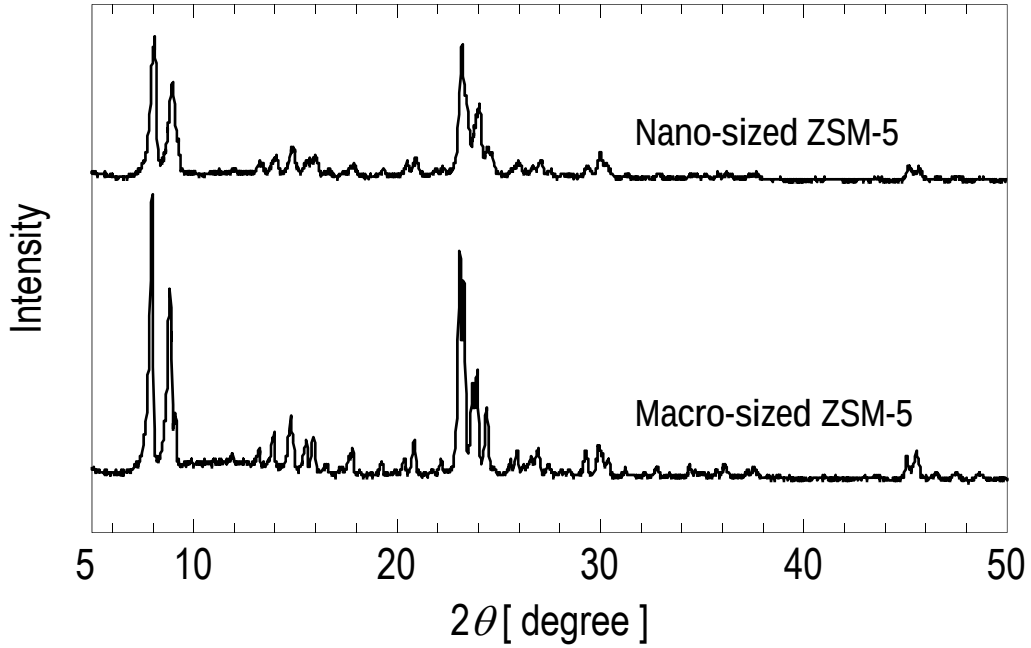

Figure 3. X-ray diffraction patterns of nano- and macro-sized ZSM-5 zeolites.

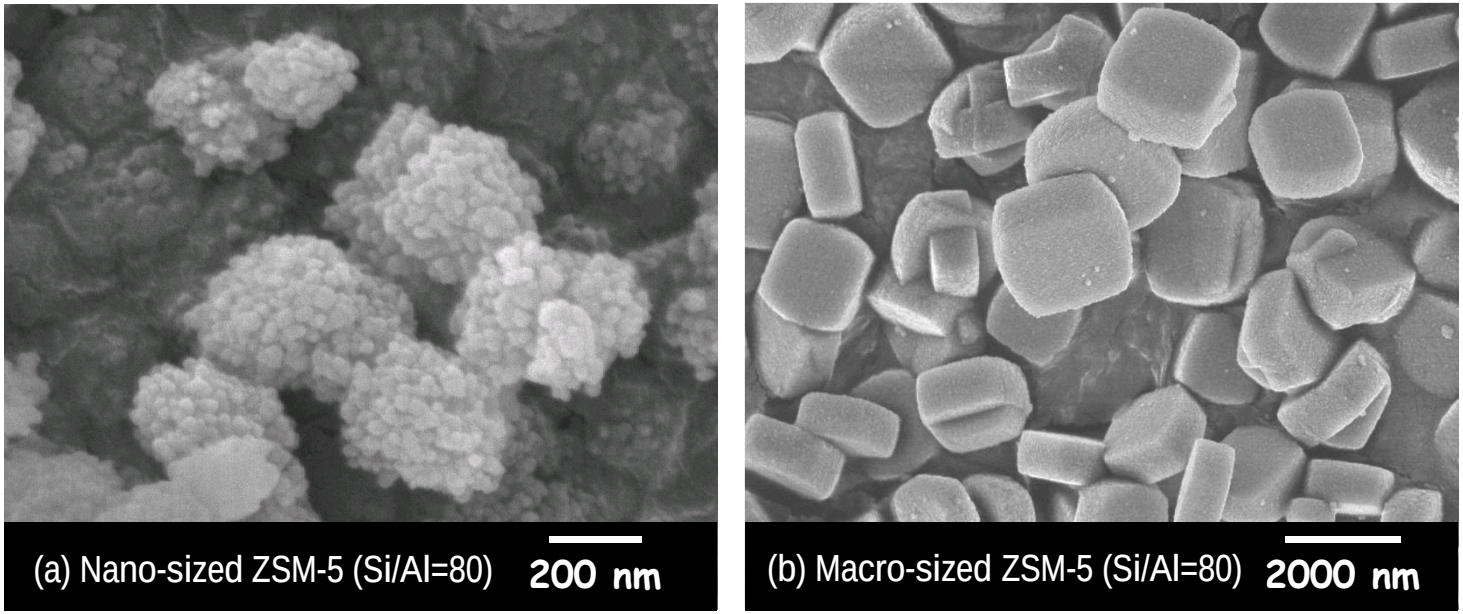

Figure 4. FE-SEM photographs of (a) nano- and (b) macro-sized ZSM-5 zeolites.

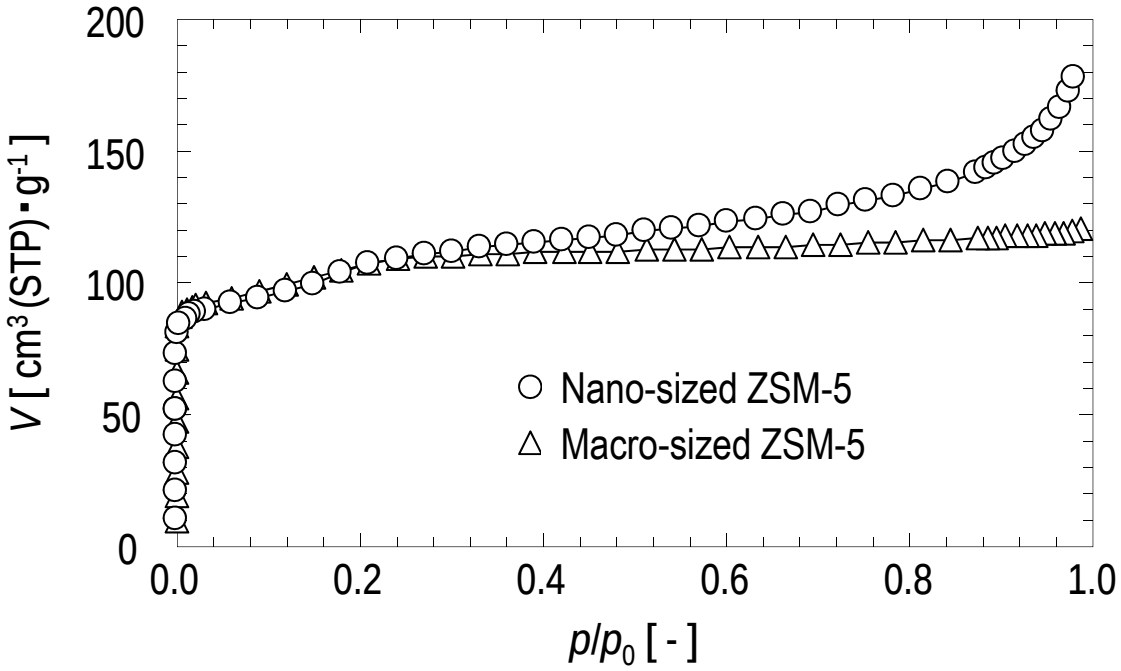

Figure 5. Nitrogen adsorption isotherms of nano- and macro-sized ZSM-5 zeolites.

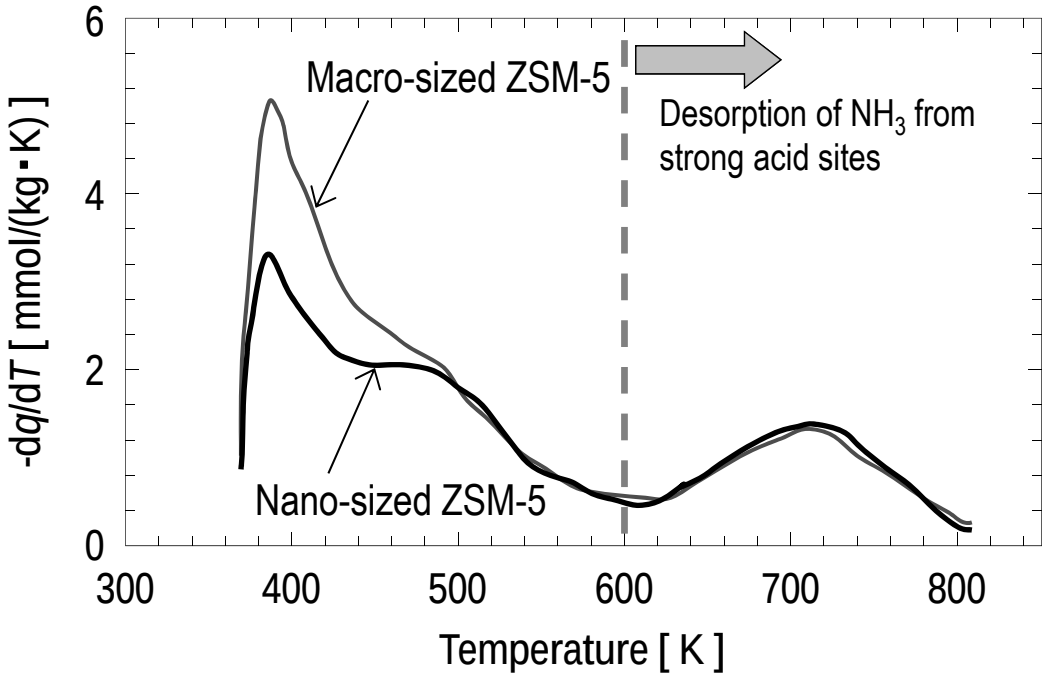

Figure 6. NH_3-TPD profiles of nano- and macro-sized ZSM-5 zeolites.

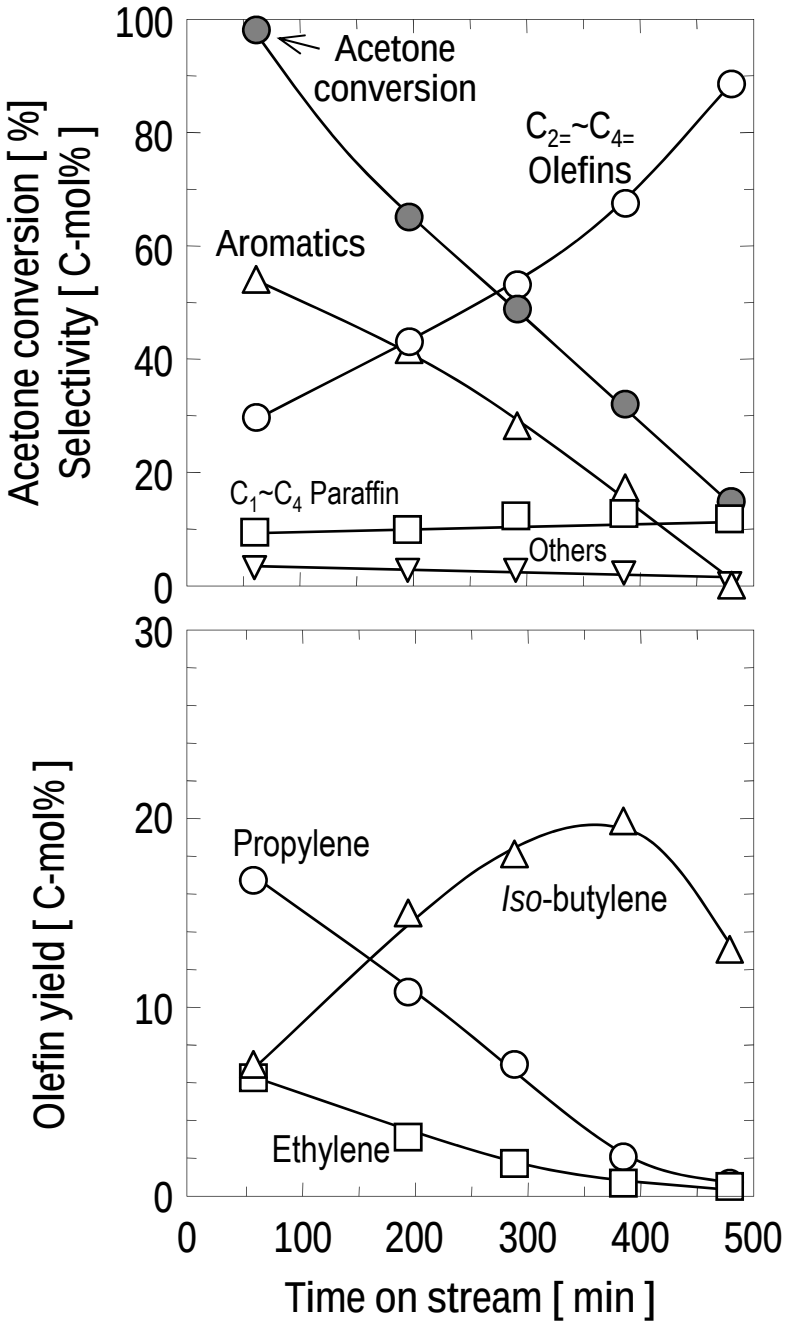

Figure 7. Changes in acetone conversion, products selectivity and olefin yield with reaction time over the macro-sized zeolite. The reaction was run at 673 K with a *W*/*F* of 0.5 kg-cat/(kg-acetone/h).

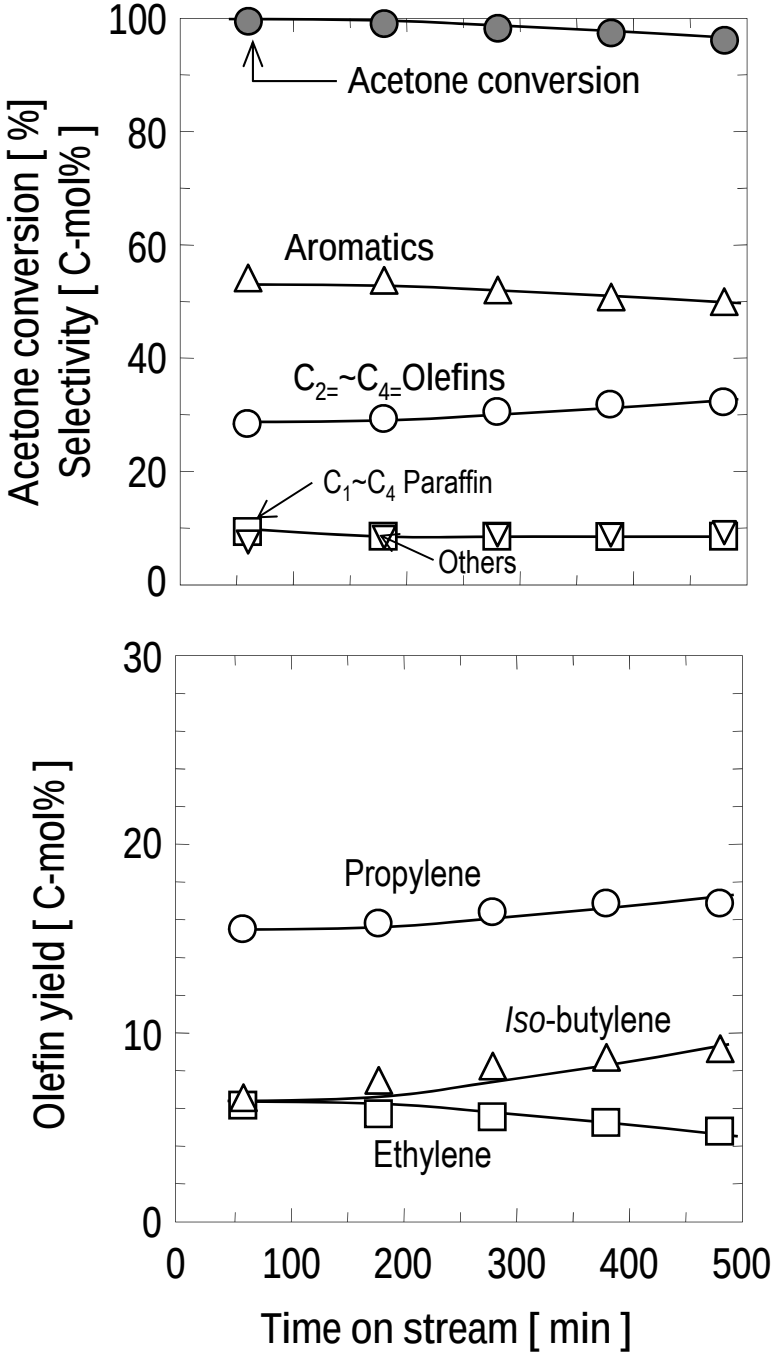

Figure 8. Changes in acetone conversion, product selectivity and olefin yield with reaction time over the nano-sized zeolite. The reaction was run at 673 K with a *W*/*F* of 0.5 kg-cat/(kg-acetone/h).

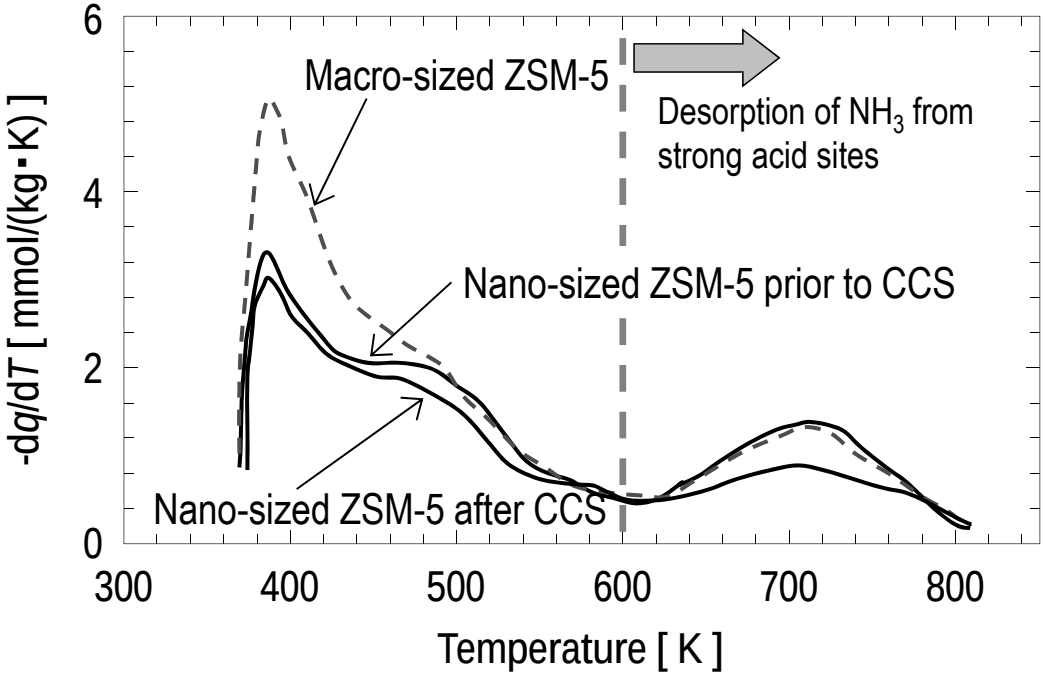

Figure 9. NH_3-TPD profiles of the nano-sized zeolite prior to and after CCS treatment.

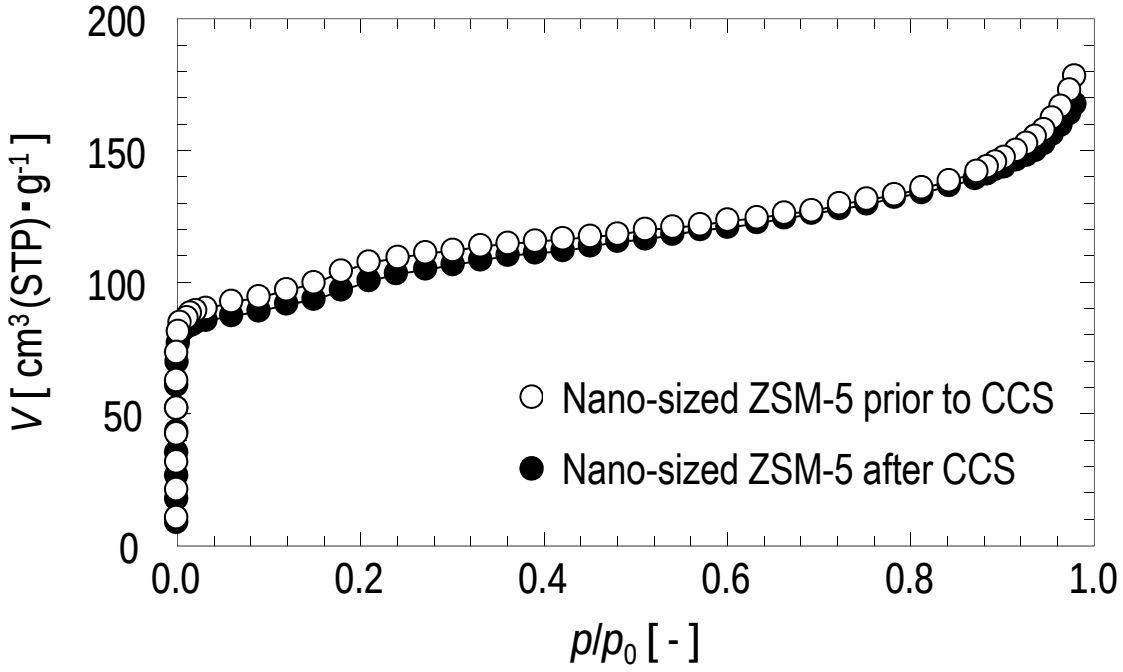

Figure 10. Nitrogen adsorption isotherms of the nano-sized zeolite prior to and after CCS treatment.

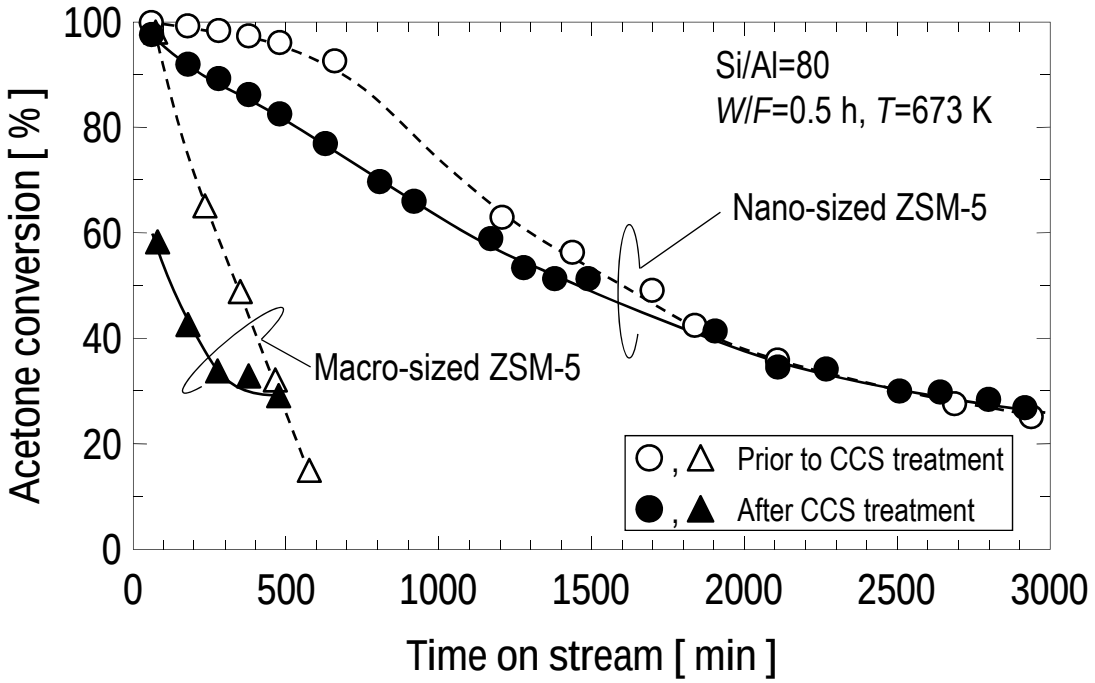

Figure 11. Change in acetone conversion with time over nano- and macro-sized zeolites prior to and after CCS treatment. The reactions were run at 673 K with a *W*/*F* of 0.5 kg-cat/(kg-acetone/h).

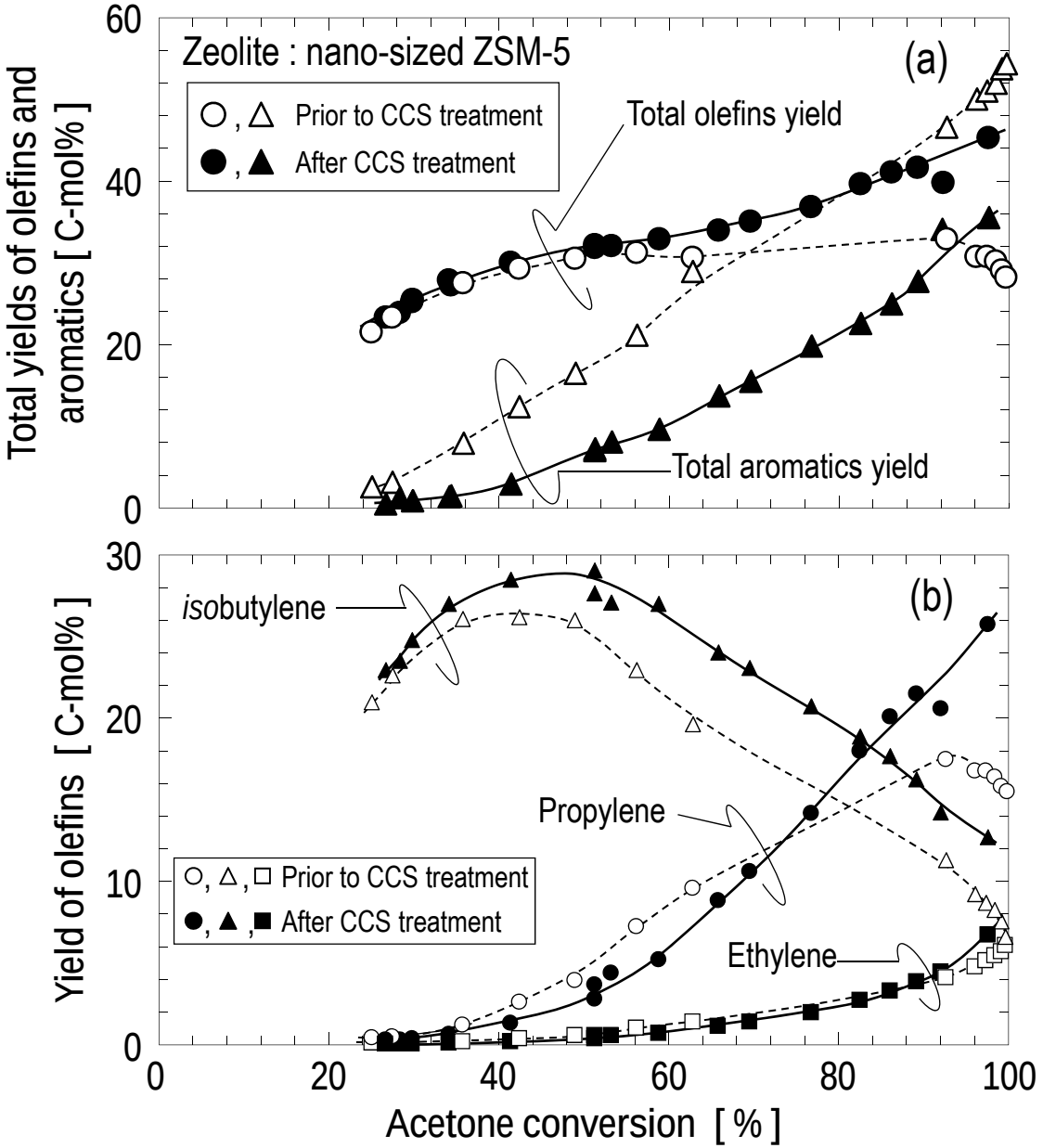

Figure 12. Relationship between acetone conversion and product yields ((a) total olefins and aromatics yields and (b) each olefin yield) during the acetone to olefins reaction over the nano-sized zeolite prior to and after CCS treatment. The reactions were run at 673 K with a *W*/*F* of 0.5 kg-cat/(kg-acetone/h).

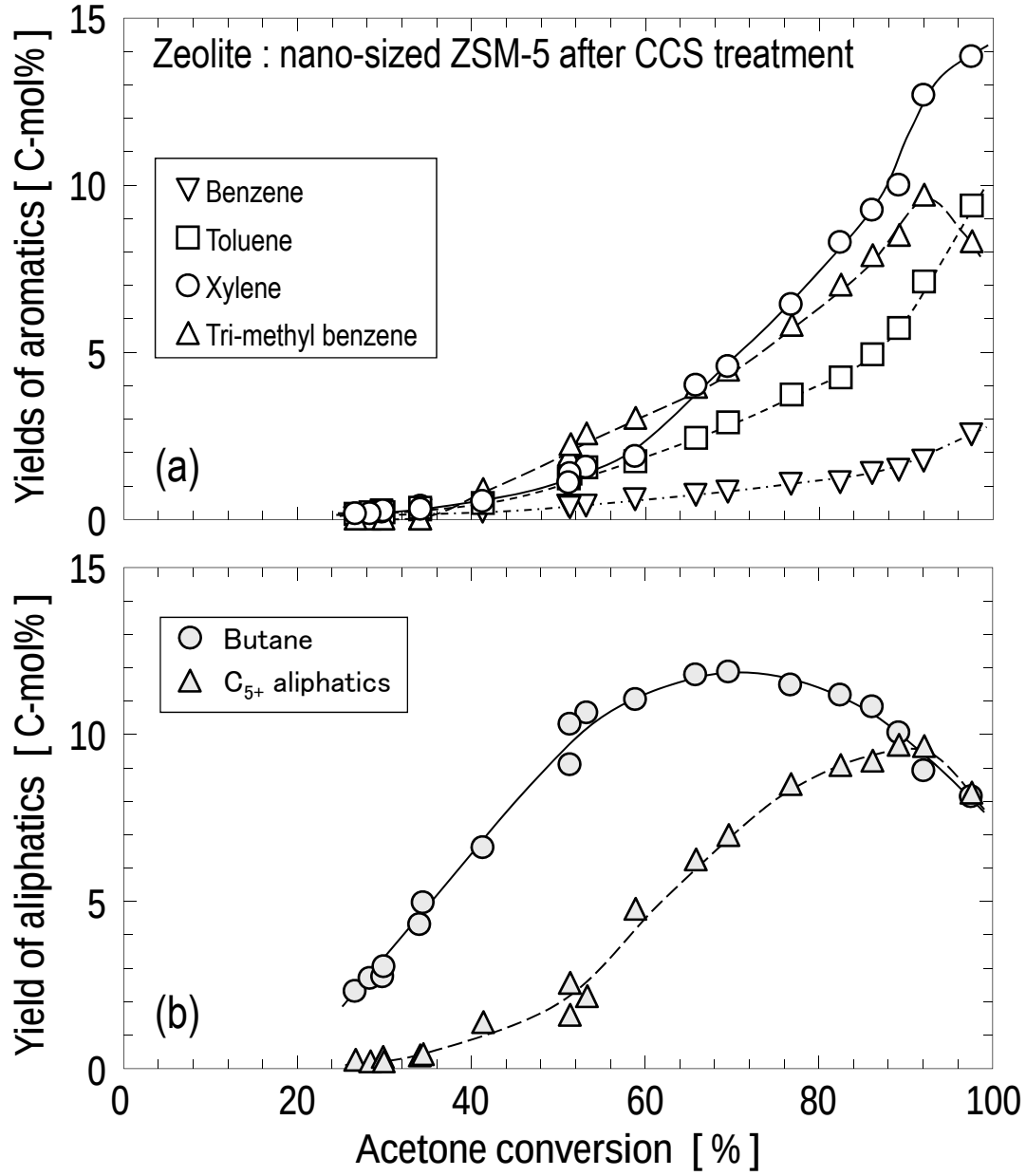

Figure 13. Relationship between acetone conversion and product yields ((a) aromatics yields and (b) aliphatics yields) during the acetone to olefins reaction over the nano-sized zeolite after CCS treatment shown in Fig. 12.

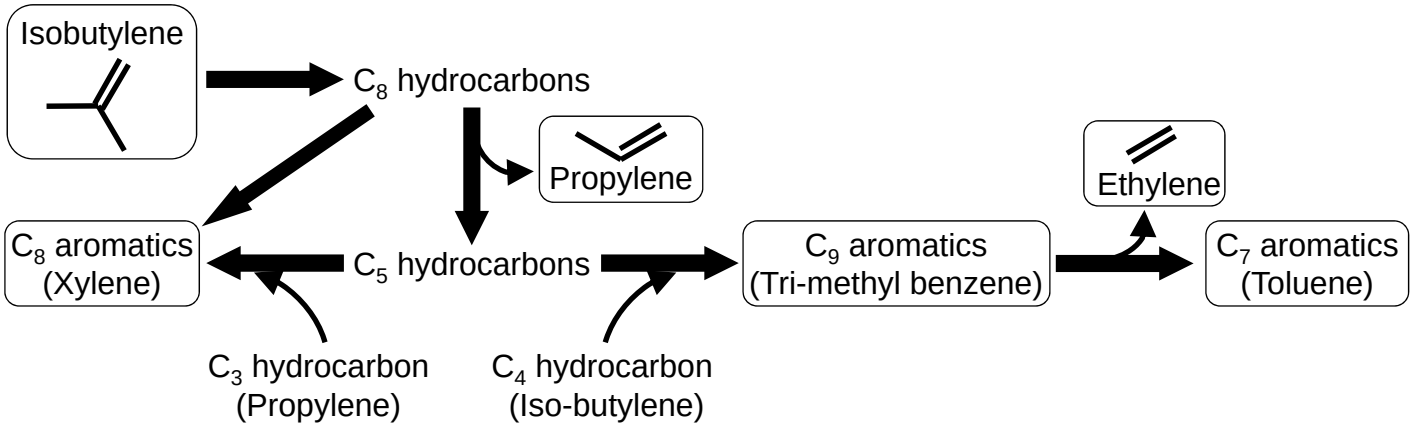

Figure 14. Possible reaction pathways for propylene, ethylene and aromatics from isobutylene.